Geometry, Geology, and Geodesy: Locating Site Features Relative to Surroundings

Dave Goss

September 9, 1989

Abstract

Several modern earth sciences techniques are applied to determine the precise location of SSC components relative to their surroundings. This note attempts to show what factors are important and the best way to proceed to locate components, taking the main ring beamlines as a major example. A method of optimizing locations via programming is discussed.

I. Introduction: Geometry

The Department of Energy (DOE) in its record of decision on January 18, 1989, confirmed the choice of the Dallas–Fort Worth, Texas (DFW) site as the approximate locale for the construction of the SSC. The site proponents were organized under the leadership of an agency of the State of Texas, the Texas National Research Laboratory Commission (TNRLC). The TNRLC had responded to the April 1989 Invitation for Site Proposals for the Superconducting Super Collider (SSC), DOE/ER-0315 (ISP). A standard plastic overlay outline of the SSC footprint was made available to site proposers and other interested parties upon request. This 1:24,000 scale plastic footprint overlay was then used by all responsive proposers to determine the location of SSC facilities relative to natural and cultural features within their proposal jurisdiction by overlaying it onto standard U.S.G.S. 7 1/2 × 7 1/2-minute topographic maps, hereafter referred to as topos or quad sheets (from quadrangle, not quadrupole). At this scale the representation of a 9.6-m-wide roadway would be 4.E-4 m or 0.4 mm across. (Fine pencil lead is 0.5 mm in diameter.) This is roughly the limiting positional accuracy of the topo maps.

Since features cannot be located on a topo to better than about 10 m and they certainly cannot be digitized any more accurately than that, a certain degree of approximation in locating SSC facilities is understood to be present at the outset. The initial specification of the site is no better than that. Real estate boundaries can usually be more accurately specified locally than that.

Site proponents all did some optimization in siting the SSC footprint within their several jurisdictions. The most important consideration was to reduce the potential impact of land acquisition for the SSC upon local homes and businesses. Even aside from the paramount moral grounds for doing so, reducing the number of homes and businesses taken by eminent domain is an important factor in maintaining local support for the SSC project. The presence of local support played an important role in the site selection.

Other obvious location considerations are to keep SSC facilities constructed on surface out of bodies of water, to keep the magnets (chiefly the quadrupoles) away from sources of vibration, to orient the main ring to utilize the advantages of the site such as transportation access or desirable (from a construction viewpoint) rock strata and to minimize the costs and problems of land acquisition. As far as reasonable, the spheres of influence of the surrounding communities should be taken into account.

The location of the main ring tunnel, experimental halls, shaft locations, booster accelerator chains and associated test beams, and major campus facilities are tied together by a particular design concept that, for brevity, I shall call a lattice. This deliberate misuse of the term by extending its meaning may prove fruitful insofar as it emphasizes the interconnectedness of the machine design.

J. R. Sanford [2] has given an account of the origins and properties of the machine footprint. In concept, the footprint is a planar oval land area outline with some projections ("ears"). The longer axis of the oval is about 30 km (29,980.738 m) long and the short axis about 25 km (24667.464 m). The land area is a strip some 304.8 m wide in the stratified fee region of the arcs. The stratified fee estate of subterranean ownership is similar in effect to a pipeline or buried cable easement, except it restricts wells and other intrusions within a larger volume than these better known examples. The fee simple areas (totally owned by DOE) are 335.38 m to 396.24 m wide over the tunnel areas, plus special land areas for the injector chain of accelerators, test beam layout, and campus surface facilities.

The local vertical projection of the footprint onto Earth's surface defines the land boundaries of the SSC. For example, suppose the footprint were tilted along its long axis by 0.25 degrees. The difference in height above a plane perpendicular to local vertical at ring center would be (30 km) sin (0.25 degrees) = 130.9 m height difference. The horizontal shortening due to raising the end of the footprint would be
30 m × [1-cos (0.25 degrees)] = 0.2856 m, less than one part in 1.0E–5, which is less

than the error specified by the Texas Society of Professional Surveyors for the accuracy of surveys of urban business districts.

Note that because of the curvature of the Earth, the center of a chord 30 km long must be

$$y = R[1 - \cos(\text{ANGLE})] \text{ with ANGLE} = \sin^{-1}(15\ \text{km}/R) \sim 15/R,$$

or

$$y = 1/2\, R\, (\text{ANGLE})^2 \sim 225\ \text{km}^2/2(6371\ \text{km}) = 0.01766\ \text{km},$$

i.e., a horizontal planar ring with extremities at the surface would be 17.7 m deep at the the center. This is a significant fraction (over 10 percent) of the height difference (130.9 m) chosen above as an illustration.

An alternative way of looking at this is to note that the ring tilted by 0.25 degrees along the long axis has its ends above and below a plane passing through the center and horizontal at that point, of ±65.45 m. However, the end elevations would be 65.45 + 17.66 = 83.1 m (upper) and –47.8 m (lower) with respect to the central elevation (check: 83.1 + 47.8 = 130.9 m).

In summary, the lessons of this simplistic analysis indicate the following:

- For most purposes, horizontal deviations of distance from the plane dimension are small enough to ignore, since 1 – cosine (angle) is second order in the angle.
- Vertical deviations go as the sine, first order in the angle, and are significant.
- Elevations of planar features must be corrected for the curvature of the Earth when lateral dimensions such as those of the SSC are involved.
- The outside of a centrally horizontal oval ring has the direction of local vertical (along Earth's radius) nowhere exactly perpendicular to the plane of the ring, i.e., the direction of "up" depends on position, if "up" is opposite the local gravitational field.

The geometry of the ring in 3-space thus emphasizes the global nature of construction for systems large enough that arcsine of the ring radius divided by Earth's radius cannot be neglected. A good measure of this is the deviation of a tangent to the Earth's surface from the arc, $y \sim x^2/2R$. For a linear distance of 11.38 km, this is 0.01 km or 10 m. For projects in which the deviation is one cm, the linear extent is 357 m, which is why the curvature of the Earth can be ignored in constructing ordinary buildings.

It might seem that the tilt (dip) of the ring might imperil the alignment of magnets and detectors. That it need not is evident from the example of LEP (at CERN), with a tilt of over a degree. Experimental areas will be built plumb with local gravity, in any case. The question then arises as to how great the angle of inclination of items internal to, viz. the solenoid in a large solenoidal detector, needs to be. I suggest that the local tilt of the beamline (always less than or equal to the ring tilt) be taken up by the alignment of the IR focusing optics, since they must include dipoles anyhow.

The slope of the tunnel magnets is a separate issue. A 13 m magnet tilted by 0.25 degrees will have one end 5.67 cm lower than the other. This is not enough drop to affect the stability of the magnet supports, unless they are awfully rickety. It might be enough drop to annoy a magnet alignment crew working with spirit levels rather than electronic distance measuring devices and modern survey techniques.

If the strike (direction of intersection of plane of the ring with local horizontal at ring center) lies along the bearing of the long axis (called the obliquity), the ring tilt at the center of the experimental halls is zero on each side of the ring. The strike is perpendicular to the dip direction, and to the projection of the dip direction on a horizontal plane. The dip angle is the angle between local horizontal at ring center and the plane of the ring, and is restricted to be less than 0.5 degrees (ISP). The pressure heads that would result from steeper local tilts of the beamline have the potential to cause cryogenic problems, such as requiring more equipment to maintain the same design operating condition.

II. Geology: What's underground and why should we care?

The SSC facilities contain three notable underground components: the main ring tunnels, the experimental halls, and the access shafts and ramps leading to these facilities. The SSC site is underlain by fairly soft sedimentary rocks that will be excavated by a variety of mechanical means. The ease (read expense) of excavation and the stability of constructed facilities depend upon the mechanical properties of these rocks, so that the location of rocks with definite characteristics is an important consideration in the design of the facility.

For design purposes, it is convenient to divide the subsurface materials into overburden and bedrock. The overburden is capped by products of weathering rich in organic material (humus) capable of supporting vegetation. This is the scientific definition of soil. Geologically such materials are called residual soils to distinguish them from stream deposits (alluvium) or material deposited downslope by the process of mass wasting (colluvium). There are alluvial deposits of up to 15 m thickness on site that are terrace deposits associated with former stream courses; most such deposits, however, are less than 6 m thick. The residual soils range in thickness from a few cm to 1.2 m.

A transition zone of weathered rock that varies from intensely fractured to massive separates the overburden from fresh unweathered bedrock below. The degree of weathering, fracturing, and organic material decreases with depth.

Sedimentary rocks consist of mineral grains cemented together by some cement which is typically microcrystalline to amorphous. Clastic rocks formed of mineral grains weathered from rock masses and transported to a particular depositional environment are classified on the basis of grain size as conglomerates and sandstone, or mudrocks (siltstones and claystones), depending on whether the typical grain size is greater or less than 62 micrometers in linear extent (size 4 sieve).

The term "clay" indicates both a size range (less then 4.0 micrometers) and a mineral family with members like kaolinite (used in making china), illite, montmorillonite, smectite, and others. Since the mineral grains almost always occur within the size range, there is little confusion except that other minerals, viz. quartz, can also be reduced to clay size particles.

Rock units have several identifiable characteristics. A "formation" is a mappable unit recognizable in outcrop, i.e., distinguishable from other units. Formations may be subdivided into members or even depositional layers like beds or laminae. A related set of formations forms a "group." A formation is often referred to a "type section" of outcrop, usually at the locality of the formation name. For example, the Eagle Ford Group is named after the Dallas suburb of Eagle Ford, at which the type section occurs as a stream cut along the Trinity River.

Sedimentary rocks are deposited in near horizontal layers called beds. The process of turning loose sediments into rocks ("lithification") typically involves the action of heat, pressure and fluids that may alter the minerals in the sediments ("diagenesis") and produce the compaction, cementation and recrystallization characteristics of the rocks produced. This typically follows burial at depth.

The depositional environment for the rocks of the site area was the near shore and shelf region of the Late Cretaceous (Gulfian) continental shallow seas that extended through the middle of the North American continent at various times, from the Gulf of Mexico to Alaska. Following deposition, these rocks were exposed to erosion during the Cenozoic era. These rocks dip toward the Gulf of Mexico at around 0.65° toward the SE (1.1–1.7 percent slope) and thicken down dip across the site. Because of the combined effects of dip and erosion, the older rocks are found on the West side of the site and the younger on the East. The oldest and deepest rocks likely to be encountered by the tunnels, halls, and shafts are the clays, thin sand layers, and limestone flags of the uppermost formation of the Eagle Ford Group called the Arcadia Park Formation. The type sections for the formation and group are in the Dallas area about 30 km North of the site. The Arcadia Park is mostly laminated organic rich clay in the site region.

The Eagle Ford rocks are overlain by the Austin Chalk, which forms the bedrock on the West side of the site. Technically, the Austin Chalk is a group, but its geotechnical properties are similar enough that it is treated as a formation in the site region, sometimes subdivided into Lower, Middle and Upper members. Above a richly fossiliferous basal region (the "fishbeds") a meter or so thick, the formation consists of fairly thick bedded limestone (mostly chalk) with thin fissile claystone (shale) partings. Some of the partings are layers of a volcanically derived clay rich in the mineral montmorillonite, called bentonite. Bentonite is used as an agent to increase density in drilling fluid ("drilling mud"). The Austin Chalk has its contemporaneous analogs in the white cliffs of Dover (equivalently, the Chalk Downs) or in the Niobrara Chalk of the northern U.S.A. The chalk particles are the microscopic calcite remains of tiny sea creatures (cocoliths).

The youngest Cretaceous formation that crops out on the site is the Ozan Formation, informally known as the Lower Taylor Marl. A marl is a calcareous (containing calcium carbonate) claystone. The Ozan formation has a calcium carbonate content in the range from about 12 percent to over 60 percent, so that it grades into chalk. It is typically slabby or blocky to massive in outcrop, but fissile ("shaley") sections also occur. East of the site, the sands and silts of the Wolfe City Formation (Middle Taylor Sands) may be found in road and stream cuts.

In general terms, the Austin Chalk is the easiest to work with in terms of ease of excavation and lack of support and cover needed. Second in terms of desirability is the Ozan Formation, with its high calcium carbonate content. A distant last is the clay of the Eagle Ford (Arcadia Park). The upper 1–20 m of this last group is low in calcium carbonate and high in montmorillonite. If allowed to dry, the surface of the clay crumbles away, a condition known as slaking. The Ozan Formation will also slake, but less rapidly. Standup time is of the order of hours or days for the Arcadia Park compared to weeks or months for the Ozan.

Montmorillonite is a swelling clay; it will accept up to 16 times its mass in water. The degree of swelling of *weathered* Ozan or Arcadia Park depends in sensitive fashion on the amount of montmorillonite relative to calcium carbonate. It is standard practice for the Texas Highway Department to treat clays with lime to prevent roadbed swelling and cracking. Because the upper Arcadia Park is low in calcium carbonate and high in montmorillonite, it has considerable potential for swelling and slaking. The stiffness of the

Arcadia Park also varies, so that a condition known as squeezing ground may occur in some regions, particularly where the clay is exposed to water as a result of construction processes.

All of these formations (Austin Chalk, Ozan, Arcadia Park) are aquitards that hinder the flow of water through them. Equivalently, the permeability of these rocks is very low. Tests run for the TNRLC give permeabilities in the range (1.6–7)E-8 cm/s for the Austin Chalk, 1.E-9 to 1.E-8 cm/s for the Ozan Formation; similar values (less than 1.E-8) are obtained for the Arcadia Park.

Table 3.5–4, reproduced from the DFW proposal (p. 30) lists representative mechanical properties of these rocks. The Austin Chalk is over an order of magnitude stiffer than the other two units (Young's deformation modulus) five or six times as resistant to crushing (uniaxial compressive strength) and considerably more resistant to slaking. The comparison between the Eagle Ford (Arcadia Park) and the Taylor (Ozan) Group rocks is biased by the selection of only unweathered samples of the former and both weathered and unweathered samples of the latter. This shows up in the absorption swell pressures. However, it is clear that the Ozan is noticeably stiffer and more resistant to crushing than the Arcadia Park.

In addition to the vertical discontinuities of the rock masses due to layering and bedding, discontinuities due to rock breakage, called fractures, also occur. If motion has occurred along a fracture between rock masses, the fracture is a "fault;" if no noticeable motion has occurred, the fracture is a joint. In addition to large-scale regional stresses that cause slip-stick or creep motion along faults, fractures may form as a result of unburial: the pressure drop due to erosion of the overlying bedrock decreases the hydrostatic pressure (rho*g*h) by reducing the depth of burial *h*. The spacing of joints formed this way may be characteristic of a given layer or even a member, and persist over lateral instances of km, except where faults are present. The density of fracture increases markedly as a fault is approached laterally; the joints may be 4 m apart at large distances from a fault or fold, and decrease to a meter of separation or less in the vicinity of a fault. Evidence for motion along a fault may be a characteristic smoothed, grooved, or gouged surface known as "slickensides." Fractures may be filled with soluble or suspendable minerals such as calcite, quartz, iron (hematite or goethite), clays or gypsum. Slickensided faults in the chalk produce characteristic "flutes" of grooved calcite fillings.

Not only do fractures permit the passage of fluids (e.g., water), they also affect the mechanical properties of the rock, notably the characteristic wave speed and alternation of the various modes of oscillation. Several problems in excavation and construction tend to be associated with fracture zones: excess water, weak rock (support required), changes in rock removal in excavation, and changes in position (height and alignment) of particular rock types. Experience indicates that excess water should not be a problem on the site, and that additional support requirements will usually be light (patterned rock bolt arrays). At least one fault is known to cross the ring alignment (near E1) and surface faults that persist at depth have a combined throw of 10–20 m over fracture zone about 30 m wide near location F10. A smaller offset of 2–10 m exists near location F1, but the fractures have not yet been located. Because of support requirements, it would be unwise to locate the experimental halls in either locale, although the zones are narrow enough that support for the tunnel should be constructible in straightforward fashion.

The faults on the site appear to be associated with the Balcones Fault Zone, which was last active in Miocene time [roughly 9 million years (9Ma) ago]. The site lies in Uniform Building Code Zone 0, the lowest category of seismic hazard. The maximum acceleration due to earth movements within the site region is anticipated to be less than 0.04 g (at the 90 percent confidence level). The main problem with the faults is that they may form through-going fractures. Many faults are known to terminate at given levels, at least within the chalk; they are not through-going. Several of the faults have healed by pressure and the deposition of calcite filling by groundwater. Examination of the walls of various quarries indicates that fractures extending more than 15 m below the weathered zone are a small percentage of the total. However, the tunnel will undoubtedly cross a number of faults. Most of these will give little problem in excavation and support. Wide fractured shear zones of the type associated with, for example, the San Andreas (CA) system do not occur on site.

Some faults within or near the site occur as the boundary fractures on down-dropped blocks called grabens, that are identified easily because they place blocks of rock higher in the stratigraphic section in contact with those lower the section; for example, the Ozan Formation is in fault contact with the Austin Chalk in a graben near the spillway of Lake Waxahachie, south of town. Other grabens occur near the town of Italy in an old landfill and near the town of Rockett on the northeast edge of the site. No grabens are known to cross the ring, but faults at F1 and F10 associated with the high rocks (horst) in the section do so. Other faults of possibly large displacement within the site include the Long Branch (stream) fault at a reservoir north of Sandis and faults crossing Bear Creek and Brusby Creek on the northern portion of the site. While there are notable fractures in the Oza Formation along Onion Creek and in the CSC commercial landfill at Avalon, the amounts of throw appear to be very small and the strata displaced less than a few tens of centimeters vertically.

Preliminary evidence from the start-up geotechnical program indicates the presence of a high spot in the Eagle Ford Group between F10 and F1. This, coupled with the depth of cover requirements and the near proximity of stream incisions at Waxahachie Creek to the Northwest, Red Oak Creek to the Northeast, and the Nelson Branch tributary to Chambers Creek in the vicinity of E9 (near Lumkins), gives the most severe constraints upon the ring geometry (considering cover requirements). Within the originally proposed footprint, it turns out that a ring dip of around 0.4 degrees is necessary if the Eagle Ford is to be avoided in both halls and tunnel and the minimum cover requirement maintained under creek crossings. Alternatively, some of the creeks might require culverting and filling.

III. Geodesy: Where in the world are we?

Geodesy is the science of location of points or phenomena or features within or upon the surface of the Earth. It is a branch of geophysics that uses the latest techniques of metrology to determine the coordinates (and sometimes the time) of geophysical events. It bears the same relation to the art of surveying that physics bears to engineering in general; it forms the scientific basis for the practical application. Recent triumphs of geodesy have included the direct observation of relative continental motion as a result of seafloor spreading using the technique of Very Long Baseline Interferometry (VLBI) astronomical measurements. Improved values (parameterization) for the figure of the Earth have resulted from precise measurements of satellite orbits combined with clever calculations. More refined calculations using seismic data plus refined gravity measurements have improved our understanding of the internal density distribution of the Earth so that constraints are placed on thermal, compositional, and flow dynamics of the Earth's interior.

Historically, geodesy has dealt largely with the angular position and height of points upon the Earth's surface, determined by astronomical and gravity measurements, supplemented by some sort of time measurement. To a zeroth approximation, the surface of the Earth is spherical in shape, and only two angles and the height above a reference sphere are required to fix the location of a point. A first approximation recognized the flattening of the Earth due to its rotation and the consequent dynamic effects. Since the actual surface of the Earth is rough and parts are covered with water or ice, the gross features of a place can be described via the gravitational forces or potentials acting there. It is apparent that a spherical harmonic expansion of the surface location will have multipole moments of arbitrarily high order because of the height differences along the surface (topography).

A rotating fluid planet in equilibrium would have its equilibrium surface as a surface of constant gravitational plus rotational potential (otherwise, mass flow would occur, and the shape would change). This notion lies behind the concept of mean (averaged over tidal and temperature effects, other changes less than a year in period) sea level, the hypothetical average level that the ocean would have if a canal were built to the place in question. However, the real Earth has angular as well as radial changes in its density distribution that produce local differences in the gravitational potential and field. This means that the mean sea level equipotential surface (the geoid) is not just a simple regular surface such as an ellipsoid. These differences in gravitational potential imply differences in height of the geoid. Therefore, features such as surface topography and contacts between geotechnical units can vary irregularly within a region, even if the strata or land surface is quite smooth and regular. An alternative description in terms of a reference ellipsoid and perpendicular height above it is possible. Because of advances in modern survey techniques, it is now possible to avoid the past dependence of location measurement on the gravitational field.

Three dimensional locations can be determined to an accuracy of a few centimeters over distances the size (30 km) of the main ring tunnel. Using Navstar Global Positioning Systems (GPS) measurements, there are presently eleven GPS satellites aloft with varying degrees of reliability that contain clocks, receivers and transmitters. The information broadcast from these transmitters includes code modulated messages broadcast on two different frequencies (L1 and L2). These transmissions include synchronized precise satellite time data, ephemeris (orbital parameter) data, pseudo-random range data, the standard positioning service (on L1) and the precise positioning service (on both L1 and L2). A number of tracking stations keep the satellites in their polar 20,183.1 km orbits in view. Ranging data from these stations sent to the master control station in Colorado Springs is used to correct the orbital parameters (interpolate and extrapolate ephemerides) of each satellite. An orbital parameters message containing atomic clock standardized time markers is sent to the satellites daily; they rebroadcast this over the L1 and L2 channels so that users may regularly update their coordinated time and orbital parameters. The user sets a GPS receiver of these radio waves over a known reference point (monument), selects the four or more satellites visible, and receives the satellite broadcasts on L1 = 1575.42 MHz and L2 = 1227.6 MHz. In practice, for centimeter accuracy, a minimum of two receivers are used; one receiver is at a known location (the base) and the other at a mobile station. This configuration is called differential positioning. Two spread spectrum waveforms are used: a 1023 kHz drip rate acquisition code (C/A) with a period code (P). The C/A code is universally available, but possibly degraded in accuracy. The navigation message from each satellite gives its orbital elements, a correction for clock reference time relative to a standard, and identifies each 6 second standard interval. An almanac message gives the approximate data for each active satellite so that all visible satellites may be found once the first is known. The system is referenced to its base station, whose coordinates are precisely known with respect to the World Geodetic System of 1984 (supersedes WGS 72). Using this information, the GPS receiver decodes satellite orbit parameters (broadcast ephemeris) as a function of time and calculates the range from the receiver antenna to each satellite transmitter. These ranges are sampled as a function of synchronized (signal) time and coupled with the known positions of all the satellites as found from the decoded ephemeris data applicable to the same time interval. The use of better satellite positions computed by various organizations (precise ephemeris) would result in even better accuracy. A computed position results from the intersection points of the ranges, after correction for time of flight. The use of two transmitting frequencies allows for the effects of the ionospheric part of the atmospheric signal delay to be taken into account, while tropospheric effects can be minimized by short base line distance between the receivers, such as would occur at the SSC site.

The GPS receiver/computer uses clock time offset, latitude, longitude and altitude in determining a three-dimensional position. In order to achieve maximum accuracy, the receiver system should be able to utilize both the standard positioning service (C/A) and the precise positioning service (P) pseudo random noise codes and the precise ephemeris. The system used in performing the GPS survey for the SSC Geotechnical Program of May-July 1989 was a set of TI-4100 GPS receivers with the capability to utilize both standard and precise positioning service codes, but used the broadcast ephemeris.

Since the satellite positions are referenced with respect to the center of the Earth, the outcome of a GPS measurement is a vector location (x, y, z) with respect to axis fixed in the center of the Earth. This is equivalent to specifying the radial distance from the center of the Earth r, the geocentric colatitude or polar angle θ and the longitude (azimuthal angle) λ. It is shown below that this is equivalent to specifying λ, the geodetic latitude ϕ and the height h above a standard reference ellipsoid.

In terms of the geocentric latitude $\psi = \pi/2 - \theta$ (warning: this is not the geodetic latitude marked on the globe) the geopotential at (r,ψ,λ) is

$$U = -\frac{GM}{r} + \frac{GMa^2}{2r^3} J_2 \,(3\sin^2\psi - 1) - \frac{1}{2}\omega^2 r^2 \cos^2\psi \tag{1}$$

with: equatorial radius $a = 6378.137$ km;

$GM = 3.986005 \times 10^{-3}\ \mathrm{m^3 s^{-2}}$

A, B, C = moments of inertia about principal axis;

ellipticity coefficient $J_2 = 1.08270 \times 10^{-3} = \dfrac{C-A}{Ma^2}$

$\omega = 0.72722 \times 10^{-4}\ \mathrm{s^{-1}}$

polar radius $c = 6356.75$ km

flattening $f \equiv (a-c)/a$

(equivalently, $c = a(1-f)$)

$f^{-1} = 298.25722$

Evaluate U at $r = a$, $\psi = 0$ (equator),

$$U_0 = -\frac{GM}{a}\left(1 + \frac{1}{2}J_2\right) - \frac{1}{2}a^2\omega^2 = \frac{GM}{c}\left[1 - J_2\left(\frac{a}{c}\right)^2\right];$$

thus

$$1 + \frac{1}{2}J_2 + \frac{1}{2}\frac{a^3\omega^2}{GM} = \frac{a}{c}\left[1 - J_2\left(\frac{a}{c}\right)^2\right] .$$

And, to first order,

$$f = \frac{3J_2}{2} + \frac{a^3\omega^2}{2GM} = 3.3579 \times 10^{-3} .$$

More accurately,

$$f = \frac{1}{298.25722} = 3.3528107 \times 10^{-3}$$

and

$$1 - f = 0.9966472$$

and

$$\delta = \frac{1-(1-f)^2}{(1-f)^2} = 6.739497 \times 10^{-3} .$$

An ellipsoid of revolution obeys the equation

$$\frac{z_0^2}{c^2} + \frac{x_0^2}{a^2} = 1 = \frac{r_0^2\cos^2\psi}{a^2} + \frac{r_0^2\sin^2\psi}{c^2} .$$

Using the flattening as defined above, the polar semi-minor axis is $c = a - af = a(1-f)$. Thus,

$$\frac{a^2}{r_0^2} = \cos^2\psi + \frac{\sin^2\psi}{(1-f)^2}$$

$$= \frac{(1-\sin^2\psi)(1-2f+f^2)+\sin^2\psi}{(1-f)^2}$$

and
$$r_0 = \frac{a}{\left[1+\sin^2\psi\,\frac{(2f-f^2)}{(1-f)^2}\right]^{1/2}} .$$

Note
$$\delta \equiv \frac{1-(1-f)^2}{(1-f)^2} = \frac{2f-f^2}{(1-f)^2}$$

so that
$$r_0 = \frac{a}{\left[1+\delta\sin^2\psi\right]^{1/2}}$$

is the expression for the reference ellipsoid in terms of the geocentric latitude ψ.

The geodetic latitude ϕ as marked on the globe is the angle between the equatorial plane and the perpendicular height h above the reference ellipsoid (Fig. 1). The angle between h and the extension of r_0 may be called μ; then $\phi = \psi + \mu$ (Fig. 1). The plane perpendicular to the ellipsoid intersects the equatorial plane at an angle γ, the complement of ϕ; $\gamma = \pi/2 - \phi$ (Fig. 1). The condition on the ellipsoid is

$$\frac{\partial z}{\partial x} = -\frac{c^2}{a^2}\cot\psi = -(1-f)^2\cot\psi$$

$$= -\tan\gamma = -\cot\phi \quad .$$

Expanding ϕ enables us to find a relation between ψ and μ:

$$(1-f)^2\frac{\cos\psi}{\sin\psi} = \frac{\cos\psi\cos\mu - \sin\psi\sin\mu}{\sin\psi\cos\mu + \cos\psi\sin\mu}$$

$$\left[(1-f)^2-1\right]\cos\psi\sin\psi\cos\mu = \sin\mu\left[\sin^2\psi + (1-f)^2\cos^2\psi\right]$$

or
$$\sin\mu\left[\frac{1-(1-f)^2}{(1-f)^2}\sin^2\psi + 1\right](1-f^2)$$

$$= \cos\mu\cos\psi\sin\psi\left[1-(1-f)^2\right] .$$

Finally, using
$$\delta = \frac{1-(1-f)^2}{(1-f)^2} \ ,$$

$$\tan \mu = \frac{\delta \cos \psi \sin \psi}{1 + \delta \sin^2 \psi} \ .$$

As an example, for $\psi = \pi/6$, $\sin \psi = 1/2$ and $\cos \psi = \sqrt{3}/2$;

$$\tan \mu = \frac{(\delta/2)(\sqrt{3}/2)}{1 + \delta/4} = \frac{\sqrt{3}}{4}\left(1 - \frac{\delta}{4} + \frac{\delta^2}{16}\right)$$

$$\tan \mu = 2.913379 \times 10^{-3}$$

$$\mu = 0.1669238 \text{ degrees}$$

$$\cos \mu = 0.9999958 \ .$$

$1 - \cos \mu = 4.2 \times 10^{-6}$, which is measurable astronomically (one thousandth of a second equals (0.001) = 2.8×10^{-7} degrees = 4.9×10^{-9} radians).

Since $\phi = \psi + \mu$, it is possible to determine ϕ and r_0 from a knowledge of the polar angle θ and the equatorial radius a and the polar radius c.

For points in the northern hemisphere, the extension of h to the polar axis intersects the axis at a point Q a distance $H = \overline{OQ}$ below Earth's center at O (Fig. 1). If the distance to the point P on the reference ellipsoid $\overline{QP}$ = R, then the radius of a parallel of latitude is

$$x_0 = r_0 \cos \psi = R \cos \phi \ .$$

The square of the eccentricity of the ellipse is

$$e^2 \equiv \frac{a^2 - c^2}{a^2} = 2f - f^2 = 1 - (1-f)^2 \ .$$

Using $$\tan \phi = \frac{1}{(1-f)^2}\frac{z}{x} = \frac{\tan \psi}{(1-f)^2} = \frac{\tan \psi}{1-e^2}$$

and $$z_0 = R \sin \phi - H = r_0 \sin \psi \ ,$$

we find $$\tan \phi = \frac{r_0 \sin \psi + H}{r_0 \cos \psi} = \tan \psi \left(1 + \frac{H}{r_0 \sin \psi}\right)$$

$$(1-e^2)^{-1} = 1 + \frac{H}{R \sin \phi - H}$$

$$(1-e^2)R \sin \phi = R \sin \phi - H$$

and finally $$H = e^2 R \sin \phi \ .$$

From Pythagoras' Theorem,

$$R^2 = (H + z_0)^2 + x_0^2 = x_0^2 + z_0^2 + 2Hz_0 + H^2$$

and $$\frac{z_0^2}{1-f^2} + x_0^2 = a^2 \qquad \text{(ellipse condition),}$$

substitute $$a^2 = (1-f)^2 R^2 \sin^2\phi + R^2 \cos^2\phi \ ;$$

$$R^2 = \frac{a^2}{1 - e^2 \sin^2\phi} \ ,$$

where $$R = \frac{a}{\left(1 - e^2 \sin^2\phi\right)^{1/2}}$$

is called the meridional radius of curvature. The latitudinal radius of curvature centered at C (Fig. 1) is

$$\rho = \frac{R^2}{a}(1-e^2) \ .$$

The total distance r associated with a location above (or below) the surface of the Earth, its associated longitude λ, and polar angle θ are equivalent to description in terms of (x, y, z) coordinates referred to a set of axes fixed in the Earth with origin at center. The geocentric latitude $\psi' = \pi/2 - \theta$ differs from the geocentric latitude of point P on the reference ellipsoid by $\Delta\psi = \psi' - \psi$ (Fig. 1 and Fig. 2). The very small angle between the normal to the ellipsoid is $\nu = \pi/2 - \beta - (\pi/2 - \mu') = \mu' - \beta$ with opposite side $t = (h\tan\beta)\sin\nu$ so that the distance increment from the small triangle is $l = t\csc(\pi/2 - \mu') = t\sec\mu'$ or $l = h\tan\beta\sin(\mu' - \beta)\sec\mu'$. By the sine law,

$$\sin\Delta\psi = (h/r)\sin\mu \quad .$$

The angle β follows from astronomical measurements,

$$\psi' = \psi + \Delta\psi, \qquad \mu' = \tan^{-1}\left(\frac{\delta\cos\psi'\sin\psi'}{1 + \delta\sin^2\psi'}\right)$$

which fixes ν and therefore l. The total distance $r = r_0(\psi') + l + h\sec\beta$ can then be generated from h and the angles. The observations would actually give β, μ', and ψ'. This fixes $r_0(\psi')$ and therefore

$$h = \frac{r - r_0(\psi')}{\sec\beta + \tan\beta\,\sec\mu'\,\sin(\mu' - \beta)} \;,$$

which gives

$$\Delta\psi = \sin^{-1}\left[\frac{h}{r}\sin\mu\right] \;,$$

which allows $\psi = \psi' - \Delta\psi$ to be found. From this, the intersection with the reference ellipsoid

$$r_0(\psi) = \frac{a}{\left(1 + \delta\sin^2\psi\right)^{1/2}}$$

and the direction of the normal to the ellipsoid

$$\mu = \tan^{-1}\left[\frac{\delta\sin\psi\cos\psi}{\left(1 + \delta\sin^2\psi\right)^{1/2}}\right]$$

finally fix the geodetic latitude $\phi = \psi + \mu$. This proves (by construction) that it is possible to determine the geodetic coordinates h, ϕ, λ, from astronomic (satellite) observations and the distance r to the point, or equivalently the vector location (x, y, z) with respect to the center of the Earth.

In addition to showing that points determined by GPS can be related to the geodesic angles plus a height above reference surface, the foregoing analysis gives the meridional or longitudinal radius R and the latitudinal radius ρ, which may be used in locating the plane of the collider ring with respect to the reference ellipsoid and hence to anything else.

The location of positions by GPS is well suited to determining ellipsoidal heights and corresponds to the reference scheme of the North American Datum of 1983 (NAD 83), which is based upon a geocentric ellipsoid rather than the local ellipsoid used in the North American Datum of 1927 (NAD 27). The geodetic coordinates (ϕ, λ) are more accurately located in NAD 83 than NAD 27, reflecting advances in positioning based upon measurement of satellites. Because heights in the NAD 83 are independent of local gravity anomalies, measurements are more easily determined to higher accuracy. To accurately determine heights in the NAD 27 system, one uses the height from the geoid. This requires the evaluation of local gravitational anomalies in order to have an accurate geoid with which to compare the local topography. These anomalies arise from density variations in subsurface rocks. Measurement of such anomalies can give significant information about density contrasts below the overlying materials, and hence of significant subsurface structures. The state plane coordinates are in meters in the NAD 83 datum while they are in American Survey feet in NAD 27. State plane coordinates (SPC) are coordinates along east and north as (x, y) corresponding to a map projection onto the reference ellipsoid (NAD 83) or the geoid (NAD 27). This unavoidably introduces distortion in mapping from a sphere to a cone or cylinder for example, so that angles and distances may not be the same in SPC grids as in actuality; further, there are projections down to the geoid and grid surface to contend with, both of which produce changes in scale. The use of SPC to locate points to within a meter was described in SSC-N-540. In such cases, the SPC coordinates are simply used as a rectangular coordinate system locally, to that degree of accuracy. While the deviations from true distances are specified in terms of the projection equations in terms of reference locations and the difference between topographic and geoidal heights, the fact that grid distances do not correspond to actual point separation distances is a source of confusion and annoyance. The SPC are useful as legal descriptions and crude position markers but are ill-suited to detailed modeling.

IV. Geometry Revisited: Frameworks in Space

The placement of the outline of the main ring and its radiation buffer zone is the main challenge in siting the SSC. The final machine alignment will be at the submillimeter level globally, at the state of the art in precision location determination. The main ring orientation in space and its adjustment with that precision are conceptually complicated enough to be worthy of discussion.

There are a number of techniques that can be used to provide analytical location of the ring position and graphic illustration of it. An ordinary engineering drawing that shows the ring with relation to the topography on a curved background is the simplest example; draw everything to scale in the way you want it, in plane (map) view and frontal view. The frontal view can be chosen to lie along strike so that the ring appears as a straight line. Distances can be accurately scaled from either view in order to find, for example, shaft depths from particular choice of obliquity (bearing of the long axis with respect to North), and strike (intersection of ring plane with the horizontal at ring center), and dip (angle between ring plane and the horizontal at ring center) angles. Greater accuracy can be obtained by use of a systematic vertical exaggeration, viz. such that $\tan\delta' = 10^3 \tan\delta$, where δ is the true dipole angle. Comparison of the plane view with map locations and the projection of obliquity and strike angles upon it serves to identify and compare points on the ring with their surface setting. This has been used by Myhrer and Goss (1989) for site modeling.

In order to utilize the graphic and analytic capabilities of modern computation, this approach has been adapted by Mike Jones (1989) for file creation and manipulation on the Intergraph (TM) system of graphics terminals. Similar techniques could be used with some other graphics hardware/software combinations. A method of generating the main ring outline is basic to this approach. The ring may be generated from an algorithm, or imported as a file in data form. The resulting ring location information is then mapped as a sequence of files by utilizing the coordinate transformations of translation and rotation from an initially specified coordinate basis (Jones, 1989).

In order to discuss the problem in general terms, independent of hardware or software and utilize the picture developed in the preceding sections, consider a model of the main ring with its center at a height h_c above the reference ellipsoid, at latitude ϕ_c and longitude λ_c. The direction locally perpendicular to the reference ellipsoid will be given by the unit vector $\hat{u}$ ("up"). Two other axes perpendicular to $\hat{u}$ and each other are taken in the northerly ($\hat{N}$) and easterly ($\hat{E}$) directions. We now use a method of generating the main ring (via file importation or algorithm) that attributes plane coordinates to the locations of ring features, after the manner of the program MAD or by giving (r, θ) or (x, y) positions of specific shafts as a table, or simply specifying the long axis orientation and a vector perpendicular to it (for specifying the ring plane). Then the main ring may be generated in, for example, a horizontal plane with northward obliquity about the center point specified. The ring may now be positioned simply by a sequence of rotations in three-space. The angles used in the desired reorientation specify the elements of the rotation matrix M such that the coordinates of the positions of the ring in (tilted) (x, y, z) coordinates with respect to ring center undergo the same transformation as column matrices as the unit vectors

$$\begin{pmatrix} \hat{x} \\ \hat{y} \\ \hat{z} \end{pmatrix} = \mathrm{M} \begin{pmatrix} \hat{E} \\ \hat{N} \\ \hat{u} \end{pmatrix} \text{ or } x_i = \mathrm{M}_{ij} u_j \qquad \text{(F1)}$$

(summation convention). The rotation matrix is simply constructed as a product of rotation matrices corresponding to rotations about specified axes. For example, a rotation about the $\hat{u}$ axis (counter-clockwise positive, right handed) by an angle σ might be chosen to align the strike of the ring along the $y(\hat{N})$ axis, and would have a rotation matrix

$$\mathrm{M}_1 = \begin{pmatrix} \cos\sigma & \sin\sigma & 0 \\ -\sin\sigma & \cos\sigma & 0 \\ 0 & 0 & 1 \end{pmatrix} \qquad \text{(F2)}$$

associated with that operation.

The next operation might be to rotate around the $\hat{N}$ axis by the dip angle δ, represented by

$$\mathrm{M}_2 = \begin{pmatrix} \cos\delta & 0 & \sin\delta \\ 0 & 1 & 0 \\ -\sin\delta & 0 & \cos\delta \end{pmatrix}. \qquad \text{(F3)}$$

This could then be followed by a rotation around the $\hat{u}$ axis by ν to orient the long axis projections at the appropriate angle with respect to $\hat{N}$

$$\mathrm{M}_3 = \begin{pmatrix} \cos\nu & \sin\nu & 0 \\ -\sin\nu & \cos\nu & 0 \\ \sigma & 0 & 1 \end{pmatrix}. \qquad \text{(F4)}$$

The net rotation is then represented by the matrix product of the three operations:

$$\mathrm{M} = \mathrm{M}_3\mathrm{M}_2\mathrm{M}_1 \qquad \text{(F5)}$$

or

$$\mathrm{M} = \begin{pmatrix} \cos\nu\cos\delta\cos\sigma - \sin\nu\sin\sigma & \cos\nu\cos\delta\sin\sigma + \sin\nu\cos\sigma & \cos\nu\sin\delta \\ -\sin\nu\cos\delta\cos\sigma - \cos\nu\sin\delta & -\sin\nu\cos\delta\sin\sigma + \cos\nu\sin\sigma & -\sin\delta\sin\nu \\ -\sin\delta\cos\sigma & -\sin\delta\sin\sigma & \cos\delta \end{pmatrix} \qquad \text{(F6)}$$

This can be used to locate any points expressed in the original system with respect to the final, or by reversing the operation to locate any points in the final systems with respect to the original $\hat{u}$, $\hat{N}$, $\hat{E}$ coordinates.

For example, the topographic and geological information can be given as points in the *uNE* system. The points of the ring in the *xyz* system (once constructed) can be determined in the *uNE* system by

$$u_i = M_{ij}^{-1} x_j = M_{ji} x_j \tag{F7}$$

(since the rotation matrix M is real orthogonal, its inverse is its transpose). In matrix form,

$$u = M^{-1} x = M^T x \quad . \tag{F8}$$

In the *uNE* system, the curved reference ellipsoid and the reference height h_A of object A with geodetic coordinates ϕ_A, λ_A can be found in terms of the rectangular Cartesian coordinates with respect to the ring center form the information above and in the previous section. If the graphics system capabilities permit, it is then possible to obtain colored perspective plots that give the illusion of three-dimensional viewing. In any case, the specification of the distances ρ and R in terms of the coordinates obtainable by GPS and optical sighting is quite straightforward.

This is not to downgrade the importance of measurements by conventional methods influenced by local gravity, which can provide an independent check on the self-consistency of these measurement techniques, and is essential for specifying distances from the geoid (mean sea level elevations). Because of the extent of the SSC main ring outline, it becomes a useful geophysical laboratory for the interplay of astronomic and gravitational measurement techniques.

While it is certainly possible to use optical and gyroscopic means to determine locations and orientations in tunnels beyond the line of sight of GPS markers, it will probably be useful to use conventional leveling devices as well. Simply because one could envisage relying only on "transferring" successive points from GPS marker down shaft and through tunnel does not necessarily mean that this would be the most accurate means of determining locations.

The business of locating points from satellite transmissions (GPS) and laser beam reflections (EDM) is still in its infancy. Significant advances in the technology of these operations will occur during the construction of the SSC. At the moment, developments in kinematic methods of locking onto the transmission of a minimum of four satellites with a mobile receiver to successively occupy several locations rapidly and with high accuracy seem particularly promising, but other techniques may also be developed (Mader and Strange, 1987). The net result will be a reduction in measurement cost that will enable us to monitor locations more easily than we determine them initially. This will aid design by monitoring, for example, possible subsidence due to regional tectonic settling or groundwater mining form the regional aquifers.

Detailed information about site locations should be stored in the global SSC database (Sybase) as suggested by Peggs (1989). However, it is probably useful to have a variety of representations of site features ranging from the simple sketches and analytic models developed here to the detailed, highly accurate and cumbersome combinations of files that are manipulated via the likes of Intergraph (TM). This note illustrates possibilities for some of these options, as well as some of the techniques for realizing them.

Acknowledgements

Special thanks to Carlos Aiken for his helpful comments and to Mark Jasper for his patience and endurance.

References

1. SSC Site Task Force, Office of Energy Research, U.S. Department of Energy, "Invitation for Site Proposals for the Superconducting Super Collider (SSC)," DOE/ER-0315, (April 1987).

2. J.R. Sanford, "A Study of the ISP Footprint," SSC-N-524, (June 1988).

3. Texas Society of Professional Surveyors, "Standards for Land Surveys," 7th ed. (1988).

4. Texas National Research Laboratory Commission, Dallas-Fort Worth Proposal, Vol. III, (August 1988).

5. D. Goss, "Specifying Site Feature Locations in Terms of State Plane Coordinates," SSC-N-540, (Sept. 1988).

6. Myhrer and Goss, (1989) in preparation.

7. M.R. Jones, Computer-Aided Design of the Digital Footprint, RTK (SSC), (July 1989).

8. S. Peggs, "A Proposal for the Development of Lattice and Footprint Databases," (July 1989).

9. G. L. Mader and W. E. Strange, "Local Crusted Deformation Monitoring Using a Kinematic GPS Technique," EOS *68*, (1987), 1236.

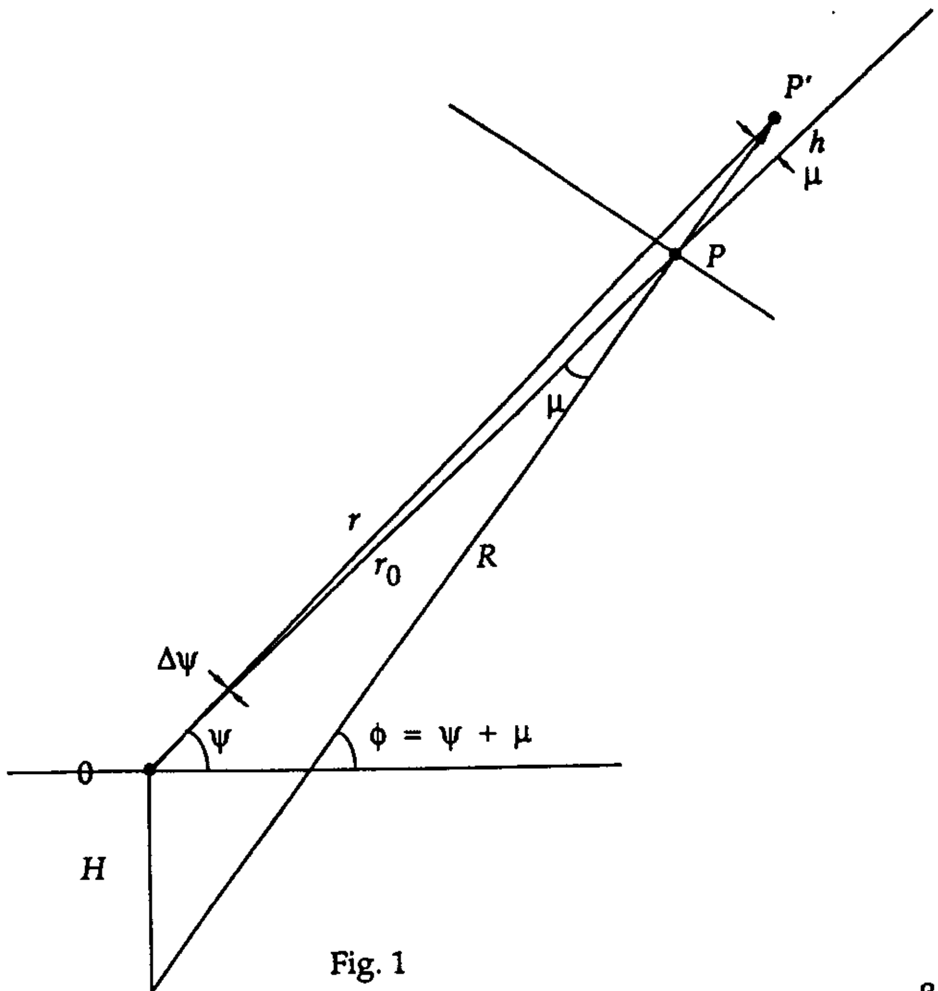

Fig. 1

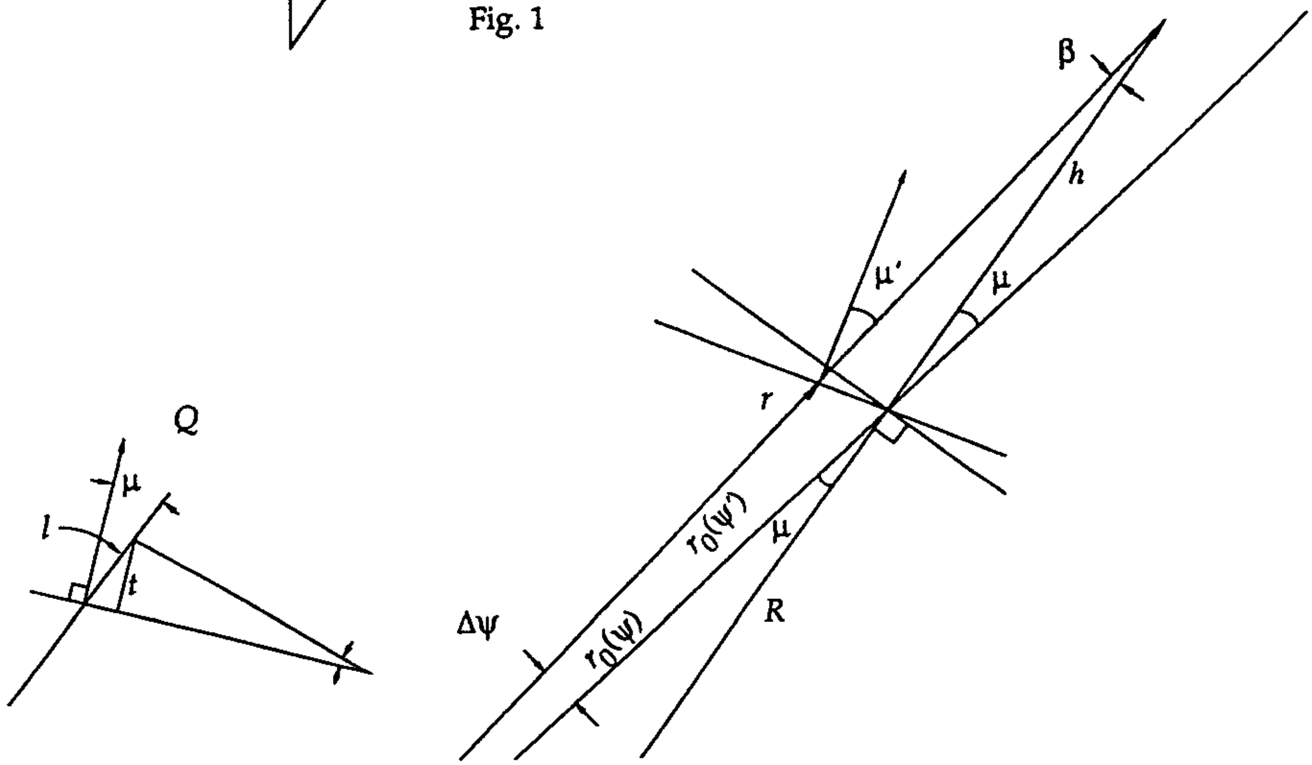

Fig. 2